

Analysis of recent VLBI catalogs

Sébastien B. Lambert

SYRTE, Observatoire de Paris, PSL Research University, CNRS, Sorbonne Universités, UPMC Univ. Paris 06, LNE
 61 av. de l'Observatoire, 75014 Paris, France
 Phone: +33 1 40 51 22 33
 E-mail: sebastien.lambert@obspm.fr

Published in [IERS Annual Report 2014](#)

1. Data sets

Eight catalogs were submitted respectively by Geoscience Australia (aus2015a/b), the Federal Agency for Cartography and Geodesy (BKG Leipzig) and Institute of Geodesy and Geoinformation of the University of Bonn (IGGB) (bkg2014a), the Space Geodesy Center (CGS) of Matera (cgs2014a), the NASA Goddard Space Flight Center (GSFC) (gsf2014a), the Institute of Applied Astronomy (IAA) of the Russian Academy of Sciences (RAS) (iaa2014a), the Paris Observatory (opa2015a), and the US Naval Observatory (usn2015a). All these catalogs provide right ascension (α) and declination (δ) of extragalactic radio sources, as well as their respective uncertainties, the correlation coefficient between α and δ , and the number of sessions and delays. Note that bkg2014a, cgs2014a, gsf2014a, opa2015a, and usn2015a were produced with the same geodetic VLBI analysis software package SOLVE developed at NASA GSFC. Both aus2015a/b and iaa2014a were produced with OCCAM.

Table 1 displays the total number of sources of each catalog, as well as the number of ICRF2 sources (out of 3414) and ICRF2 defining sources (out of 295). Some catalogs do not provide values for one or two defining sources, likely because they do not process a few sessions that were present in the session list processed to generate the ICRF2 catalog. We recommend that in the future, the analysis centers pay attention to their session list in order to get values for all 295 ICRF2 defining sources. As well, none of the catalogs provide values for all 3414 ICRF2 sources.

The median error reported in Table 1 reveals an error in declination larger than in right ascension by a factor of ~ 1.5 . The error is substantially smaller for SOLVE solutions. The smaller error for cgs2014a is likely originating in the fact that the solution provides only well observed sources with low positional standard error.

2. Frame orientation

We evaluate the consistency of the submitted catalogs with the ICRF2 by modeling the coordinate difference (in the sense catalog minus ICRF2) by a 6-parameter transformation as used at the IERS ICRS PC in previous comparisons:

$$\begin{aligned} A1 \tan \delta \cos \alpha + A2 \operatorname{tg} \delta \sin \alpha - A3 + DA (\delta - \delta_0) &= \Delta\alpha, \\ -A1 \sin \alpha + A2 \cos \alpha + DD (\delta - \delta_0) + BD &= \Delta\delta, \end{aligned}$$

where $A1$, $A2$, $A3$ are rotation angles around the X, Y, and Z axes of the celestial reference frame, respectively, DA and DD represent linear variations with the declination (which origin δ_0 can be arbitrarily chosen but was set to zero in this study), BD is a bias in declination, and $\Delta\alpha$ and $\Delta\delta$ are coordinate differences between the studied and the ICRF2 catalogs. The 6 parameters were fitted by weighted least squares to the coordinate difference of the defining sources (upper part of Table 2) and ICRF2 sources (lower part of Table 2) found in the catalog. The standard deviation of the offsets to ICRF2 after removal of the systematics of Table 2 is reported in Table 3 together with the median offset.

Though rotations around the X-axis (angle $A1$) remain almost statistically non significant (within 3 sigmas), all catalogs show significant misorientation around $A2$ larger than $10 \mu\text{as}$ (4 sigmas). We note also that solutions aus2015a/b show significant misorientation of the frame around the Z-axis close to $50 \mu\text{as}$ whereas it remains reasonable for other catalogs. The largest deviation from ICRF2 axes is observed for the bias in declination. Values BD are indeed significantly larger than those reported in the 2014 Annual Report for solutions bkg2013a and opa2013a (to be compared to bkg2014a, and opa2015a, respectively). Generally, all SOLVE solutions have declination biases larger than $30 \mu\text{as}$ in absolute value, which is significantly larger than the ICRF2 axis stability of $10 \mu\text{as}$ measured at the time

of the ICRF2 release in 2009 (Fey et al. 2015). This fact may indicate some systematics in source declinations with respect to solutions of the previous years.

3. Zonal errors

Figure 1 displays the offset to ICRF2 (in the sense catalog minus ICRF2) averaged over declination bins of 5 degrees. Solutions opa2015a, usn2015a, and bkg2014a exhibit zonal errors characterized by large declination offsets at low declinations, which may reflect the large values of BD found in the coordinate difference to ICRF2. A similar effect is also visible but less pronounced for cgs2014a and gsf2014a.

4. Standard error and noise

Figure 2 illustrates how the overall formal error, defined as the square root of $\sigma_{\alpha\cos\delta}^2 + \sigma_{\delta}^2 + c\sigma_{\alpha\cos\delta}\sigma_{\alpha\delta}$ where σ is the formal error listed in the catalogs and c is the correlation coefficient between estimates of α and δ as provided in the catalogs, varies with the number N of observations. The circled dots represent defining sources. The figure for aus2015a clearly shows that the defining sources have underestimated formal errors likely due to an overconstrained solution. (As stated in the technical document delivered with the catalog, a strong no-net rotation condition imposed to these sources.) The formal error of the same sources in solution aus2015b, in which the no-net rotation condition is less severe, appears to be at a level comparable to other sources.

Figure 2 also shows how the error on delays is propagated to the estimated source coordinates. For white noise measurements, the formal error on source coordinates is expected to decrease as $N^{-0.5}$. The figure reveals that this regime exists for N between ~ 100 and ~ 10000 . For N lower than a hundred observations (e.g., VCS sources or sources observed in only one session) the formal error varies as N^{-1} . Beyond 10000 observations, the formal error generally tends towards a limit lower than $\sim 10 \mu\text{as}$. Such a deviation is visible for all catalogs except aus2015a/b for which the formal error seems to continue to decrease closely to $N^{-0.5}$. The deviation for large N observed for all other catalogs is likely the signature of non-Gaussian correlated errors: as N increases, thermal baseline-dependent error tends to zero and the station-dependent error arising from time- and space-correlated parameters becomes dominant (see, e.g., Gipson 2006 or Romero-Wolf et al. 2012; see also Lambert 2014).

A last test was performed to assess the consistency between the formal errors and the offset to ICRF2. This test was motivated by the consideration that, although the ICRF2 is not the “truth”, it nevertheless provides accurate values of well-observed sources. As a consequence, for most of the sources, the addition of new observations after 2009 should not perturb significantly the estimated position but only improve the formal error. Figure 3 displays the scatter around the ICRF2 position computed for bins of increasing formal error. For a white noise, one should get values close to the first diagonal (i.e., the formal error fully explains the offset to ICRF2). For formal errors lower than 0.1 mas, one sees that the scatter is over the diagonal, indicating a possible underestimation of the formal errors. To quantify this scale factor, one can estimate it together with an error floor so that a realistic error Er (i.e., that explains the observed offset to ICRF2) is given by

$$Er = ((E s)^2 + f^2)^{-0.5}$$

where E is the error, s a scale factor and f a noise floor. Values of s and f estimated over sources whose offset to ICRF2 is smaller than 1 mas are reported in Table 4. Uncertainties are $\sim 10 \mu\text{as}$ on s and ~ 0.01 on f . SOLVE solutions tend to have scale factors larger than unity while OCCAM catalogs have scale factors smaller than 1. Note that the noise floor does not represent the catalog internal error since one considers the offset to ICRF2: the quantity f therefore contains the internal noise of the ICRF2. The global noise lies between 50 and 120 μas . If one assumes 40 μas for the ICRF2 internal noise (Fey et al. 2015), it means that the analyzed catalog internal noises are larger by a factor between 1 and 3.

5. Conclusions and recommendations

The above results lead to some recommendations for analysis centers who plan new submissions in the future. First, it is recommended to include all ICRF2 sessions in the processed session list, in order to get values of, at least, all 3414 ICRF2 sources. Second, analysis centers should focus on understanding several points: (i) the significant systematics in orientation ($\sim 50 \mu\text{as}$) showing up in Table 2, (ii) the zonal errors appearing in Fig. 1 for some solutions, and (iii) the non-Gaussian errors dominating for large number of observations raised by Fig. 3. About the latter item, one should understand particularly why aus2015a/b OCCAM solutions decreases differently than SOLVE catalogs for larger numbers of delays. In the future, the correction of this defect should be achieved by better modeling and parameterization of clock and troposphere correlated errors.

Table 1. Number of sources by categories and median error. Unit is μs . Values for right ascension are corrected from the cosine of the declination.

	----- No. Sources -----			-- Median Error --	
	Total	ICRF2	Def	RA	Dec
aus2015a	3383	3170	295	676.5	965.0
aus2015b	3406	3191	295	576.0	817.0
bkg2014a	3340	3110	294	281.4	429.4
cgs2014a	969	961	294	44.3	50.1
gsf2014a	3740	3408	294	264.0	400.0
iaa2014a	2946	2799	293	445.6	690.3
opa2015a	3684	3378	295	283.5	440.2
usn2015a	4048	3410	295	230.0	333.3

Table 2. Rotation parameters with respect to ICRF2. A1, A2, A3 and BD are in μs . DA and DD are in μs per degree.

	A1	A2	A3	DA	DD	BD

Defining sources						

aus2015a	2.2	20.9	49.0	-0.2	-0.4	-10.8
+-	3.7	3.7	3.4	0.1	0.1	3.5
aus2015b	1.7	28.9	52.6	-0.7	-0.5	-17.9
+-	3.9	3.9	3.6	0.1	0.1	3.8
bkg2014a	6.4	13.9	-12.6	0.2	0.9	-53.0
+-	3.5	3.4	3.1	0.1	0.1	3.4
cgs2014a	8.6	19.1	-12.1	0.1	0.1	39.6
+-	3.5	3.5	3.2	0.1	0.1	3.5
gsf2014a	-4.6	11.4	-8.8	0.1	0.6	-38.1
+-	3.4	3.4	3.0	0.1	0.1	3.3
iaa2014a	-3.9	12.1	-1.1	-0.1	0.5	1.0
+-	3.7	3.6	3.4	0.1	0.1	3.7
opa2015a	-8.9	18.9	-3.3	0.1	1.0	-57.8
+-	3.4	3.4	3.1	0.1	0.1	3.3
usn2015a	-9.1	18.1	-2.3	0.2	0.9	-50.9
+-	3.4	3.4	3.1	0.1	0.1	3.3

All common sources						

aus2015a	10.0	14.1	38.0	-0.0	-0.3	-6.0
+-	4.4	4.5	4.1	0.2	0.1	4.1
aus2015b	15.7	25.9	38.4	-0.6	-0.4	-15.8
+-	4.7	4.8	4.5	0.2	0.1	4.4
bkg2014a	10.5	16.5	-13.0	0.2	1.0	-53.7
+-	4.5	4.6	4.2	0.2	0.1	4.3
cgs2014a	10.4	18.8	-9.2	0.2	0.3	37.9
+-	4.5	4.6	4.2	0.2	0.1	4.3
gsf2014a	-2.3	14.5	-8.2	0.1	0.7	-36.0
+-	4.5	4.6	4.2	0.2	0.1	4.2
iaa2014a	-0.9	11.3	-1.8	0.1	0.6	-1.7
+-	4.7	4.8	4.4	0.2	0.1	4.6
opa2015a	-3.8	18.7	-8.7	0.1	1.1	-56.3
+-	4.5	4.6	4.2	0.2	0.1	4.2
usn2015a	-4.5	21.2	-8.5	0.0	1.1	-53.4
+-	4.5	4.6	4.2	0.2	0.1	4.2

Table 3. Statistics after removal of systematics given in Tables 2. Unit is μs . Values for right ascension are corrected from the cosine of the declination.

	---- Standard Deviation ----				----- Median Offset -----			
	- Defining -		---- All ----		- Defining -		---- All ----	
	RA	Dec	RA	Dec	RA	Dec	RA	Dec
aus2015a	165.0	130.4	165.3	132.1	256.4	419.6	267.9	427.4
aus2015b	68.8	69.2	107.2	119.2	261.1	495.4	264.9	409.8
bkg2014a	48.3	59.4	401.2	419.1	117.3	223.1	118.9	211.4
cgs2014a	47.8	58.9	282.1	520.5	48.9	72.4	50.7	67.0
gsf2014a	48.7	57.1	517.9	771.1	78.7	143.8	79.1	132.8
iaa2014a	49.6	60.9	310.6	304.3	35.6	34.7	180.6	253.5
opa2015a	56.6	62.2	491.5	718.6	51.8	76.5	54.7	82.5
usn2015a	56.7	63.1	546.1	774.4	119.4	232.8	124.6	219.2

Table 4. Noise floor and scale factor estimated for sources with offset lower than 1 mas. Unit is μs . Values for right ascension are corrected from the cosine of the declination.

	-- Floor --		-- Scale --	
	RA	Dec	RA	Dec
aus2015a	97.3	117.5	0.79	0.79
aus2015b	70.4	71.2	0.96	0.93
bkg2014a	45.6	62.5	1.26	1.11
cgs2014a	36.4	48.7	2.70	2.38
gsf2014a	47.7	60.3	1.14	1.06
iaa2014a	44.4	52.1	0.99	0.83
opa2015a	50.8	62.4	1.27	1.11
usn2015a	53.7	65.6	1.67	1.47

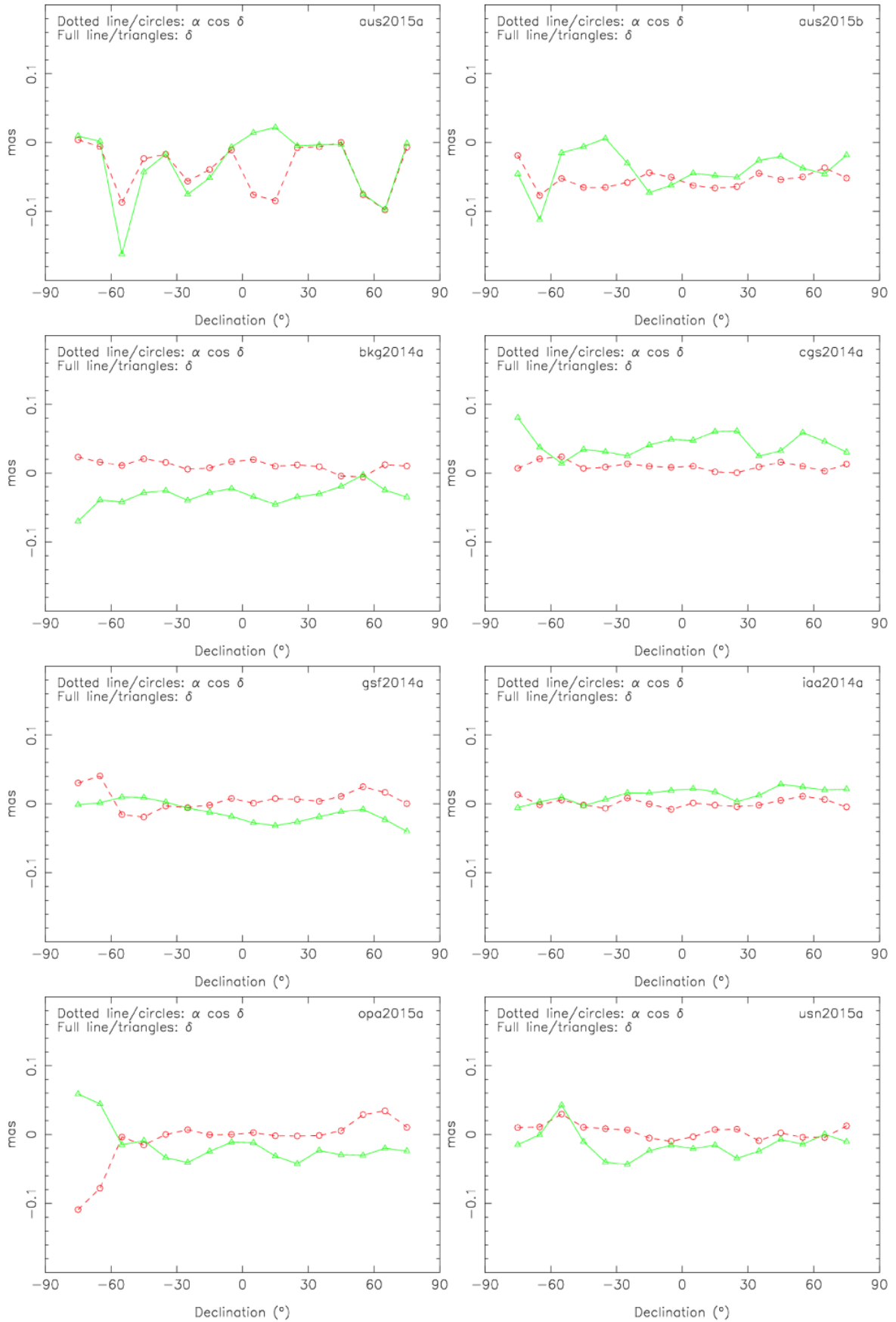


Fig. 1. Offset to ICRF2 for right ascension (dotted line with circles) and declination (full line with triangles) by bins of declination of 5 degrees.

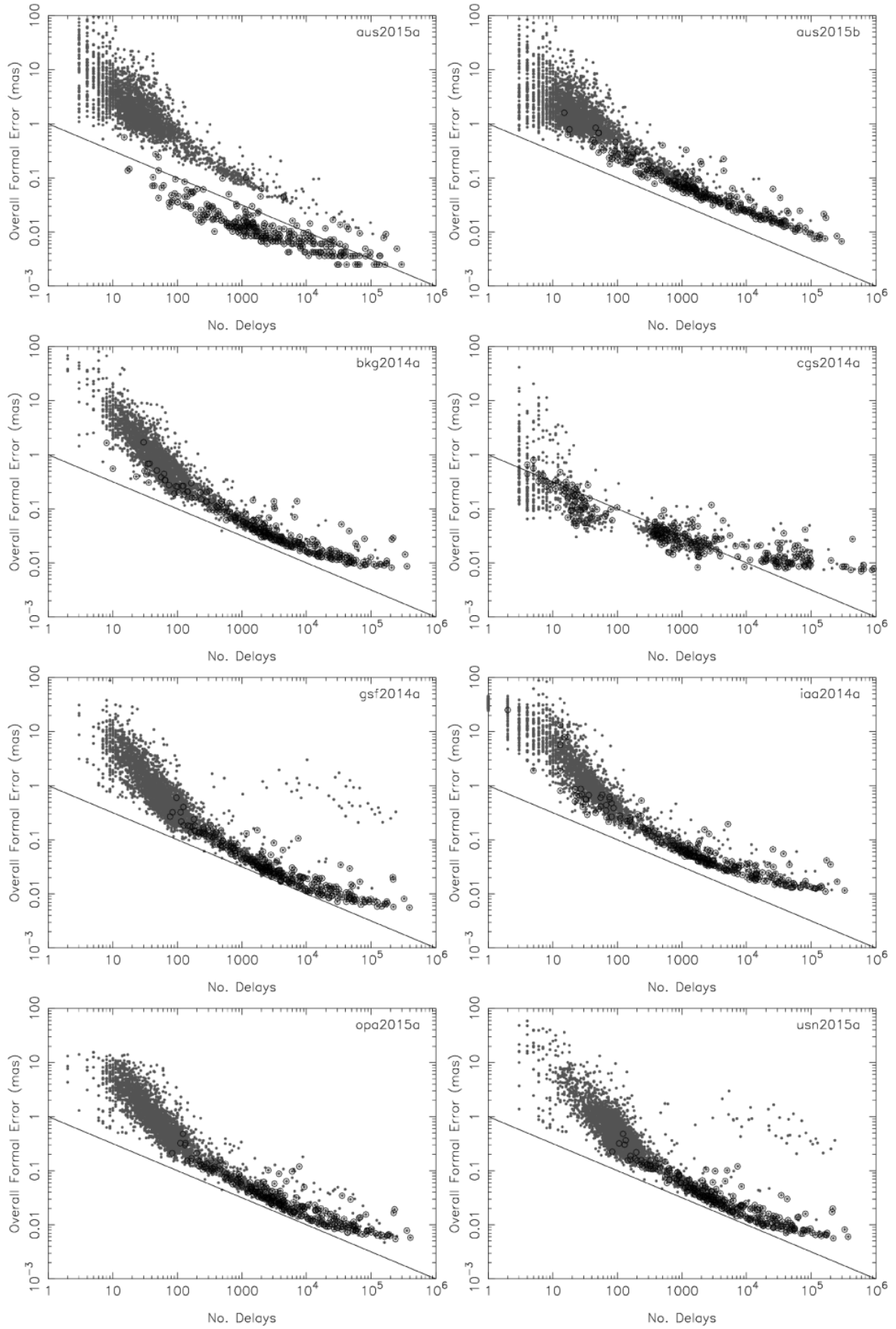


Fig. 2. Overall formal error as a function of the number of observations. The circled dots represent defining sources. The solid line indicates a decrease as $N^{-1/2}$ where N is the number of delays.

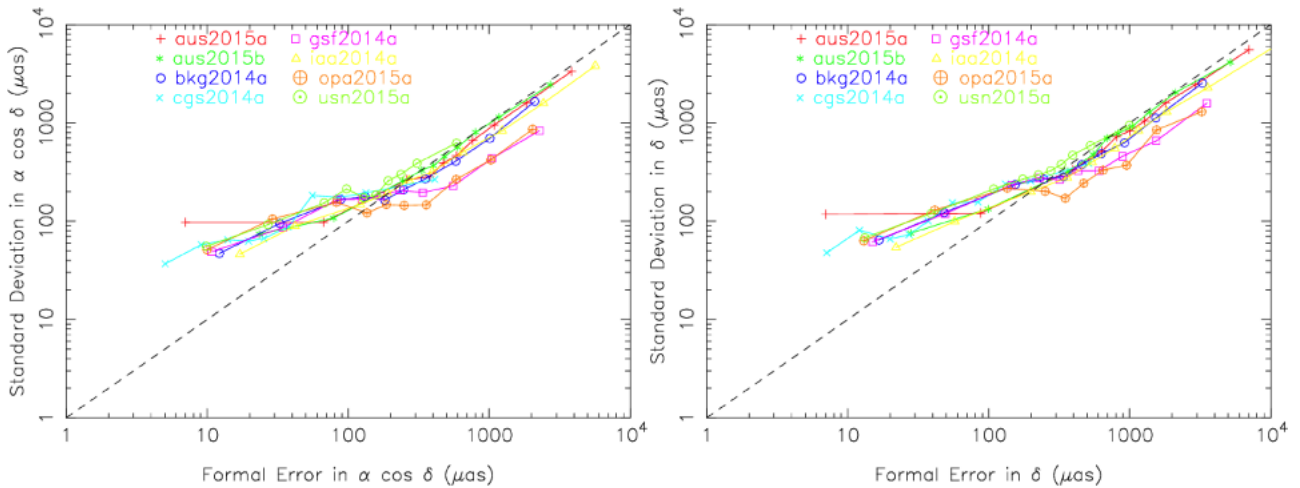


Fig. 3. Scatter of the offset to ICRF2 versus the formal error.

6. References

Fey, A. L., Gordon, D., Jacobs, C. S., Ma, C., Gaume, R. A., Arias, E. F., Bianco, G., Boboltz, D. A., Böckmann, S., Böhm, J., Bolotin, S., Charlot, P., Collioud, A., Engelhardt, G., Gipson, J., Gontier, A.-M., Heinkelmann, R., Kurdubov, S., Lambert, S., Lytvyn, S., MacMillan, D. S., Malkin, Z., Nothnagel, A., Ojha, R., Skurikhina, E., Sokolova, J., Souchay, J., Sovers, O. J., Tesmer, V., Titov, O., Wang, G., & Zharov, V. 2015, The second realisation of the International Celestial Reference Frame by very long baseline interferometry, *Astron. J.*, 150, 58

Gipson, J. M. 2006, in *International VLBI Service for Geodesy and Astrometry (IVS) 2006 General Meeting Proceedings*, NASA/CP-2006-214140, eds. D. Behrend, & K. D. Baver, 286

Lambert, S. 2014, Comparison of VLBI radio source catalogs, *Astron. Astrophys.*, 570, 108

Romero-Wolf, A., Jacobs, C. S., & Ratcliff, J. T. 2012, in *International VLBI Service for Geodesy and Astrometry (IVS) 2012 General Meeting Proceedings*, NASA/CP-2012-217504, eds. D. Behrend, & K. D. Baver, 231